Wide Area Phase Angle Measurements for Islanding Detection - An Adaptive Nonlinear Approach

Xueqin Liu, *Member, IEEE,* Jason. M. Kennedy, David. M. Laverty, *Member, IEEE,* D. John Morrow, *Member, IEEE and* Seán McLoone, *Senior Member, IEEE*

***Abstract*—The integration of an ever growing proportion of large scale distributed renewable generation has increased the probability of maloperation of the traditional RoCoF and vector shift relays. With reduced inertia due to non-synchronous penetration in a power grid, system wide disturbances have forced the utility industry to design advanced protection schemes to prevent system degradation and avoid cascading outages leading to widespread blackouts. This paper explores a novel adaptive nonlinear approach applied to islanding detection, based on wide area phase angle measurements. This is challenging, since the voltage phase angles from different locations exhibit not only strong nonlinear but also time-varying characteristics. The adaptive nonlinear technique, called moving window kernel principal component analysis is proposed to model the time-varying and nonlinear trends in the voltage phase angle data. The effectiveness of the technique is exemplified using both DigSilent simulated cases and real test cases recorded from the Great Britain and Ireland power systems by the OpenPMU project.**

***Index Terms*—Islanding detection, kernel principal component analysis, moving window, phase angle measurements, wide area protection.**

I. Introduction

Electrical energy is one of the cornerstones of our economy and our modern society has become heavily dependent on its continuous availability. Driven by a desire to deliver an affordable, secure and clean energy supply, the UK and the Republic of Ireland (RoI) are working towards achieving 15% and 40% energy generation from renewable sources by 2020, respectively. As presented in the annual global status report [1], as of early 2014 targets were in place in 144 countries worldwide for the increased deployment of renewable energy.

The ever increasing penetration of distributed renewable generation brings many technical challenges for the safe operation, protection and stability of the power grid. Power grids were historically designed assuming active power flows from high voltage to low voltage grids. This assumption is often not valid for systems with significant distributed renewable generation and consequently existing protection systems may no longer be appropriate. At the same time, the system has reduced system inertia due to increased penetration of non-synchronous generation sources (such as wind power generation, DC interconnectors and domestic PV installations) resulting in increased risk of frequency instability [1]. Taking the combined Northern Ireland (NI) and Republic of Ireland power grid as an example, the system operator often operates with an instantaneous wind penetration as high as 50%. Frequency stability is a significant issue in a small island grid due to low system inertias, where large frequency deviations after a disturbance are more likely to occur and may cause cascading trips of anti-islanding relays (such as RoCoF and vector shift protection) [2], and subsequently uncontrolled islanding operation. To reduce nuisance tripping, the RoCoF threshold is often increased [2], with an inevitable increase in the 'non-detection zone'.

In the literature, numerous islanding detection techniques have been explored. A detailed review can be found in [3] and our previous work [4]. From an anti-islanding protection and system security perspective, a reliable and fast islanding detection algorithm without nuisance tripping and non-detection zone, is still recognized as an ongoing challenge since reported techniques are not entirely satisfactory [5].

Since the first prototype phasor measurement units (PMUs) were developed by Virginia Tech in 1988, system-wide networked PMUs have been rapidly deployed in the last few years. As a consequence, a vast amount of GPS-based time-stamped data is being collected 10 to 60 times per second. The potential for real-time tracking of system dynamics afforded by synchronized phasor measurements [6], together with advanced communication and data analysis techniques, offers a novel opportunity to improve wide area protection and islanding detection performance for the evolving power grid.

Multivariate statistical approaches, including principal component analysis (PCA) and its non-Gaussian extension, independent component analysis (ICA), have been extensively applied in various fields, including image processing, statistical process control, data compression, signal processing, and fault detection. In recent years, these techniques are increasingly being considered in the electric power research area, due to the availability of synchronized PMU data and the desire to extract useful information from these data efficiently. Applications of these techniques in power systems involve islanding detection [4], [7], [8], dimensionality reduction for event analysis [9] and wind power production [10], disturbance detection [11], system coherence identification [12], [13], and oscillation monitoring [14].

X. Liu, D. M. Laverty, D. J. Morrow, S. McLoone are with the School of Electronics, Electrical Engineering and Computer Science, Queen's University Belfast, Belfast, BT9 5AH, U.K. (e-mail: x.liu@qub.ac.uk)

J. M. Kennedy is with System Operator for Northern Ireland (SONI Ltd.), Belfast, BT6 9RT, U.K.

Our previous paper [4] presented a linear PCA-based approach to islanding detection using wide area frequency measurements as a powerful tool for identifying and distinguishing between islanding events and non-islanding events. It provides a comprehensive interpretation of how and why different statistical indices derived from the PCA model represent different types of event, and offers a solid foundation for further exploration of frequency-based event analysis using recursive PCA [8], moving window PCA [15], and probabilistic PCA [7]. Unfortunately, the frequency based method suffers from a non-detection zone, making it ill-suited for islanding detection when the frequency difference between the islanding site and the other sites is small. The phase angle, as the decisive indicator of a phasor, is a vital variable for determining the state and operation of a power system [6] and may provide an alternative and complementary solution to a frequency-based approach [7]. In contrast to the frequency variable, which is a universal system parameter and exhibits Gaussian and linear characteristics, phase angle variables exhibit significant *localized*, *nonlinear* and *time-varying* characteristics [4], [7].

To handle the nonlinearity in process monitoring, numerous studies on nonlinear extensions of PCA have been investigated in the literature. Examples include principal curves based [16], multi-layer auto-associative neural network based (ANNs) [17], and the kernel function approach [18], [19]. Nonlinear extensions of the PCA, which rely on multi-layer ANNs and principal curves require solutions to nonlinear optimization problems and are prone to local minima. It has been well recognized that Kernel PCA is a popular nonlinear extension of linear PCA and a powerful tool for handling nonlinear system dynamics. For adaptive time-varying process monitoring, a recursive or a moving window approach is often adopted. Recursive approach [20], [21], which updates the model for a growing data set that includes new samples without excluding the old ones, may have difficulties to implement in practice.

To capture the nonlinear and time-varying characteristics simultaneously and achieve enhanced anti-islanding protection, this paper proposes the use of an adaptive nonlinear method, called moving window kernel principal component analysis (KPCA), to investigate multiple phase angle measurements across the whole power system. As the window slides along the data, a new nonlinear model is built by including the newest sample and removing the oldest one. While a number of algorithmic developments have been reported to update and downdate the models efficiently [22], [23], their computational accuracy may be compromised. To present the basic concept of adaptive KPCA, which is promising for islanding protection, the traditional moving window approach is used in this paper.

To summarize, although PCA-based approaches for islanding detection utilizing frequency measurements have been successfully applied to islanding detection, some significant issues remain and deserve further investigation: (1) frequency-based passive approaches inevitably introduce a non-detection zone; (2) PCA assumes linear interrelationships between variables, which hampers its application if the examined relationships are nonlinear and time-varying.

This paper addresses the first issue by analyzing phase angles measured from multiple different locations across a wide area simultaneously. When a system is islanded, the phase angle of the islanded system drifts away from the main power system. The phase angle difference approach between two different locations for islanding detection has been proved effective in the literature [6], [25], [26], [27]. However, issues may arise with the existing approach due to its critical dependence on the reference phase angle, as well as a fixed pre-set threshold. In this paper, multiple locations are employed in case the reference site fails or becomes islanded itself. The concept of utilizing multiple PMU locations to improve the tracking capabilities of power system dynamics has been published recently for power system inter-area oscillation monitoring [24]. To the best of our knowledge, analyzing the phase angle difference from multiple locations simultaneously, with an ‘adaptive multiple cross-reference’ approach, has not been studied previously in the islanding protection domain. It is worth noting that references [5] and [33] proposed an accumulated phase angle drift approach with a predetermined threshold setting, and demonstrated its sensitivity to small active power imbalance conditions. Again, the reliability of this approach is affected by generator inertia, power imbalance and the frequency estimation method employed, thus a pre-set threshold may not be adequate to describe a complex phase angle increase.

The second issue is addressed through the development of a nonlinear adaptive kernel PCA based multiple phase angle analysis technique for islanding detection. This is motivated by the fact that phase angle measurements possess significant nonlinear and time-varying characteristics, due to the evolving power grid generating unpredictable fluctuations and dynamics. More specifically, changes can occur in the mean and variance of individual variables and also in the correlation structure among variables across different locations [7]. Thus, the reliability of a traditional islanding detection methodology, using a fixed model, a pre-set threshold, and a ‘single reference’ is questionable. It may lead to undesired miss detection or false operation of islanding protection relays.

The objective of this paper is to present the first application of an adaptive nonlinear technique to synchronized wide area phase angle measurements for anti-islanding protection. The proposed ‘adaptive protection’ methodology makes several contributions and its novelty is multi-fold: (1) the nonlinear and time-varying characteristics of phase angles are captured and reflected by a nonlinear model - Kernel PCA; (2) the threshold for islanding detection is adaptively changing; (3) the threshold is determined by statistical inference with confidence limits derived from the proposed nonlinear model; (4) multiple locations with ‘cross-reference’ are examined simultaneously; (5) the effectiveness of the proposed methodology is validated through simulated synthetic data as well as real industry data collected from two independent real power systems, representing different penetration levels of distributed renewable generation. To highlight, the ability to adaptively tune the islanding detection threshold based on the moving window kernel PCA is novel.

Although various data-mining based pattern recognition techniques have been extensively studied in the literature, such as support vector machines [28], Bayesian methods [29], probabilistic neural networks [28], fuzzy-rule based method [30], and decision trees [31], [32]. These studies focus on classifying events based on supervised learning on numerous *simulated* event data and relying on accurate labelling in order to train the classifier. Unfortunately, it is very hard to guarantee different types of event data are available for training due to their low probability of occurrence, e.g. islanding events. The advantage of the proposed method is that it introduces a one-class unsupervised learning for islanding detection, where the model is trained only based on abundant normal data. In addition, the existing data-mining methods for threshold settings often rely on a *mixture* of input parameters (e.g. up to eleven in [31]) feeding into a classifier, including the frequency, the voltage variations, rate of change of frequency and rate of change of power etc. This mixture of input parameters and the black-box nature of the classifier makes it difficult to interpret the physical meaning of the methodology. Besides, other power system events, such as generator trips also produce disturbances in the voltage, frequency, and angles similar to those generated by islanding events. Unlike the above, the proposed method focuses on phase angle alone, providing a simple physical interpretation for differentiating islanding and non-islanding events.

The remainder of the paper is organized as follows. In Section II, the moving window kernel PCA algorithm used to detect an islanded system and the implementation procedure of the proposed scheme is explained. Section III provides details of the case study phase angle measurements obtained from multiple locations on the Great Britain (GB) and Ireland power networks, and also results from simulated synthetic data. A comparative analysis of different islanding protection methodologies is also given. Then in Section IV an analysis of 'cross reference' phase angle data with and without islanding events from the two power networks is presented to demonstrate the effectiveness of the proposed method. Discussions and conclusions are summarized in Section V.

II. Methodology of Adaptive Nonlinear Approach

A. Moving Window Kernel Principal Component Analysis of Phase Angle Difference Data

The main idea of KPCA is to first construct a nonlinear mapping from an input space to a higher-dimensional feature space and then apply linear PCA in the feature space [19]. A key advantage of KPCA over other nonlinear PCA techniques (e.g. neural network based PCA) is that it does not require the solution of a nonlinear optimization problem. Instead, it is obtained as the solution to an eigenvalue problem. Additionally, since KPCA can use different types of kernel function, it can handle a wide range of nonlinearities [19].

Let $\widehat{\boldsymbol{\theta}}_i \in \mathcal{R}^n$ denote a sample vector storing n phase angle difference variables across different sites at the ith sample instant and let $M > n$ be the number of samples. KPCA maps $\widehat{\boldsymbol{\theta}} \in \mathcal{R}^n$ into a high-dimensional feature space $\boldsymbol{\Phi}(\widehat{\boldsymbol{\theta}}) \in \mathcal{F}$ and performs linear PCA in that space. The sample covariance matrix in the feature space can be written as [27]

$$\boldsymbol{\Sigma}_{\boldsymbol{\Phi}} = \frac{1}{M-1}\sum_{i=1}^{M}\left(\boldsymbol{\Phi}(\widehat{\boldsymbol{\theta}}_i) - \mathbf{m}_{\boldsymbol{\Phi}}\right)\left(\boldsymbol{\Phi}(\widehat{\boldsymbol{\theta}}_i) - \mathbf{m}_{\boldsymbol{\Phi}}\right)^T = \frac{1}{M-1}\bar{\boldsymbol{\Phi}}(\boldsymbol{\Theta})\bar{\boldsymbol{\Phi}}^{\boldsymbol{T}}(\boldsymbol{\Theta}), \quad (1)$$

where $\mathbf{m}_{\boldsymbol{\Phi}} = \frac{1}{M}\boldsymbol{\Phi}(\boldsymbol{\Theta})\mathbf{I}_M$, $\mathbf{I}_M$ is an M dimensional vector of ones and $\boldsymbol{\Phi}(\boldsymbol{\Theta}) = [\boldsymbol{\Phi}(\widehat{\boldsymbol{\theta}}_1), \boldsymbol{\Phi}(\widehat{\boldsymbol{\theta}}_2), \dots, \boldsymbol{\Phi}(\widehat{\boldsymbol{\theta}}_M)]$. $\bar{\boldsymbol{\Phi}}(\boldsymbol{\Theta}) = \boldsymbol{\Phi}(\boldsymbol{\Theta}) - \frac{1}{M}\boldsymbol{\Phi}(\boldsymbol{\Theta})\mathbf{E}_M$, $\mathbf{E}_M = \mathbf{I}_M\mathbf{I}_M{}^{\boldsymbol{T}}$, is the mean centered feature matrix and the phase angle difference matrix $\boldsymbol{\Theta} = \left[\widehat{\boldsymbol{\theta}}_1, \widehat{\boldsymbol{\theta}}_2, \dots, \widehat{\boldsymbol{\theta}}_M\right] \in \mathcal{R}^{n\times M}$. Thus, an eigenvalue de-composition of $\boldsymbol{\Sigma}_{\boldsymbol{\Phi}}$ is given by

$$\boldsymbol{\Sigma}_{\boldsymbol{\Phi}}\mathbf{u}_k = \frac{1}{M-1}\bar{\boldsymbol{\Phi}}(\boldsymbol{\Theta})\bar{\boldsymbol{\Phi}}^{\boldsymbol{T}}(\boldsymbol{\Theta})\mathbf{u}_k = \lambda_k\mathbf{u}_k, k = 1,2, \dots, M, \quad (2)$$

where λ_k and $\mathbf{u}_k$ are the kth eigenvalue-eigenvector of $\boldsymbol{\Sigma}_{\boldsymbol{\Phi}}$.

Given that the mapping function $\boldsymbol{\Phi}(\widehat{\boldsymbol{\theta}})$ is unknown, KPCA solves the eigenvalue problem of the centered Gram matrix $\mathbf{G} = \bar{\boldsymbol{\Phi}}^{\boldsymbol{T}}(\boldsymbol{\Theta})\bar{\boldsymbol{\Phi}}(\boldsymbol{\Theta}) \in \mathcal{R}^{M\times M}$,

$$\bar{\boldsymbol{\Phi}}^{\boldsymbol{T}}(\boldsymbol{\Theta})\bar{\boldsymbol{\Phi}}(\boldsymbol{\Theta})\mathbf{v}_k = \boldsymbol{\varsigma}_k\mathbf{v}_k, \quad (3)$$

where $\boldsymbol{\varsigma}_k \in \mathcal{R}$ and $\mathbf{v}_k \in \mathcal{R}^M$ are the kth eigenvalue and eigenvector of $\mathbf{G}$. Multiplying (3) with $\bar{\boldsymbol{\Phi}}(\boldsymbol{\Theta})$ produces:

$$\lambda_k = \frac{\varsigma_k}{\mathrm{M}-1}, \quad \mathbf{u}_k = \frac{\bar{\boldsymbol{\Phi}}(\boldsymbol{\Theta})\mathbf{v}_k}{\|\bar{\boldsymbol{\Phi}}(\boldsymbol{\Theta})\mathbf{v}_k\|} = \frac{\bar{\boldsymbol{\Phi}}(\boldsymbol{\Theta})\mathbf{v}_k}{\sqrt{\mathbf{v}_k{}^T\,\bar{\boldsymbol{\Phi}}^{\boldsymbol{T}}(\boldsymbol{\Theta})\,\bar{\boldsymbol{\Phi}}(\boldsymbol{\Theta})\mathbf{v}_k}} \quad (4)$$

Defining the kernel function $K(\widehat{\boldsymbol{\theta}}_{i,}\widehat{\boldsymbol{\theta}}_j) = \boldsymbol{\Phi}^{\boldsymbol{T}}(\widehat{\boldsymbol{\theta}}_i)\boldsymbol{\Phi}(\widehat{\boldsymbol{\theta}}_j)$, the centered Gram matrix $\mathbf{G}$ can be computed as

$$\mathbf{G} = \mathbf{K} - \frac{1}{M}\mathbf{K}\mathbf{E}_M - \frac{1}{M}\mathbf{E}_M\mathbf{K} + \frac{1}{M^2}\mathbf{K}\mathbf{E}_M\mathbf{K}, \quad (5)$$

where the kernel matrix $\mathbf{K} = \boldsymbol{\Phi}^{\boldsymbol{T}}(\boldsymbol{\Theta})\boldsymbol{\Phi}(\boldsymbol{\Theta}) \in \mathcal{R}^{M\times M}$, with its i,j^{th}element defined as $K(\widehat{\boldsymbol{\theta}}_{i,}\widehat{\boldsymbol{\theta}}_j)$. This approach is based on the assumption that the scalar products $K(\widehat{\boldsymbol{\theta}}_{i,}\widehat{\boldsymbol{\theta}}_j)$ can be approximated by kernel formulations, such as polynomial, RBF and sigmoid kernel functions. After constructing the PCA model in the feature space, the KPCA score vector $\mathbf{t} \in \mathcal{R}^r$, for a new sample $\widehat{\boldsymbol{\theta}}$ is:

$$\mathbf{t} = \mathbf{U}^T\bar{\boldsymbol{\Phi}}(\widehat{\boldsymbol{\theta}}) = \mathbf{A}^T\left[\mathbf{k}(\boldsymbol{\Theta}, \widehat{\boldsymbol{\theta}}) - \frac{1}{M}\mathbf{K}\mathbf{E}_M\right]. \quad (6)$$

where $\bar{\boldsymbol{\Phi}}(\widehat{\boldsymbol{\theta}}) = \boldsymbol{\Phi}(\widehat{\boldsymbol{\theta}}) - \mathbf{m}_{\boldsymbol{\Phi}}$, $\mathbf{U} = \left[\mathbf{u}_{1,}\mathbf{u}_{2,} \dots, \mathbf{u}_r\right] \in \mathcal{F}$, r is the number of retained principal components (PCs),$\mathbf{k}(\boldsymbol{\Theta}, \widehat{\boldsymbol{\theta}}) \in \mathcal{R}^M$ is the kernel vector, and

$$\mathbf{A} = \left[\mathbf{I} - \frac{1}{M}\mathbf{E}_M\right]\mathbf{V} \in \mathcal{R}^{M\times r}, \mathbf{V} = \left[\frac{\mathbf{v}_1}{\sqrt{\varsigma_1}}, \frac{\mathbf{v}_2}{\sqrt{\varsigma_2}}, \dots \frac{\mathbf{v}_r}{\sqrt{\varsigma_r}}\right] \in \mathcal{R}^{M\times r},$$

$$\mathbf{k}(\boldsymbol{\Theta}, \widehat{\boldsymbol{\theta}}) = \left[K(\widehat{\boldsymbol{\theta}}_{1,}\widehat{\boldsymbol{\theta}}), K(\widehat{\boldsymbol{\theta}}_{2,}\widehat{\boldsymbol{\theta}}), \dots, K(\widehat{\boldsymbol{\theta}}_{M,}\widehat{\boldsymbol{\theta}})\right]^T.$$

For islanding detection purposes, KPCA relies on evaluating a Hotelling's T^2 and a residual Q statistic

$$T^2 = \mathbf{t}^T\boldsymbol{\Lambda}^{-1}\mathbf{t}$$
$$Q = K(\widehat{\boldsymbol{\theta}}, \widehat{\boldsymbol{\theta}}) - \frac{2}{M}\mathbf{1}_M^T\mathbf{k}(\boldsymbol{\Theta}, \widehat{\boldsymbol{\theta}}) + \frac{1}{M^2}\mathbf{1}_M^T\mathbf{K}\mathbf{1}_M - \mathbf{t}^T\mathbf{t} \quad (7)$$

where $\boldsymbol{\Lambda}$ is a diagonal matrix storing the variances of the score variables. The confidence limits for the Hotelling's T^2 and Q

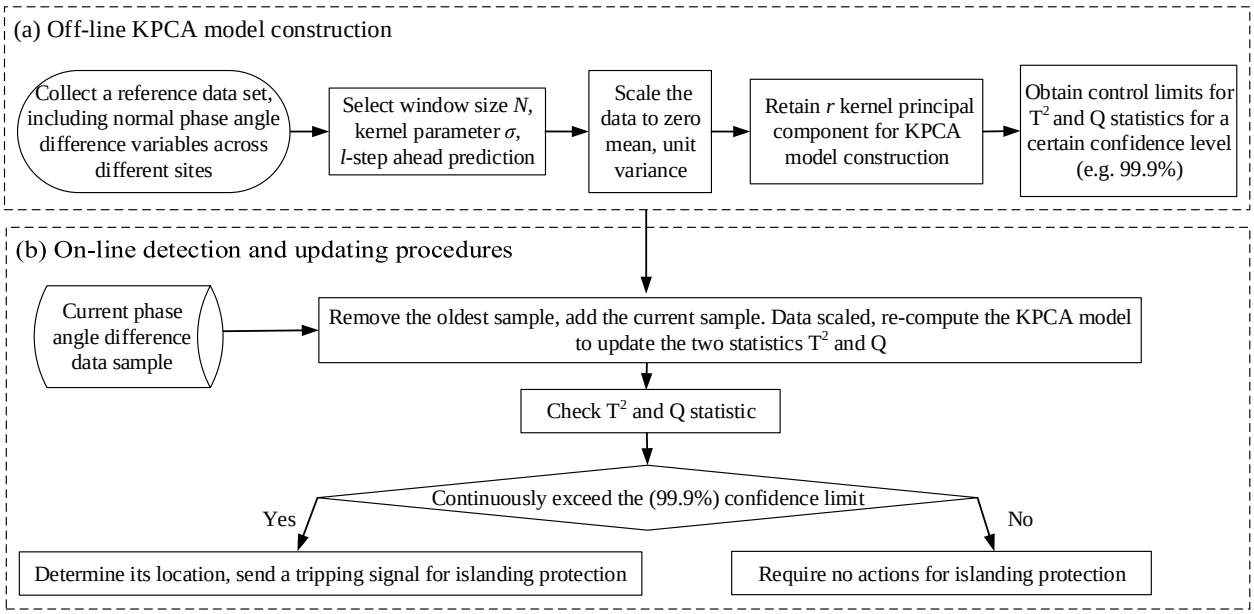

Fig. 1. A flowchart of the proposed Moving Window KPCA method for islanding protection

statistics can be calculated based on [34]. The Hotelling's statistic represents a significant variation of the phase angle difference in the KPCA model plane and the Q statistic represents a model mismatch. If either of these two statistics is above the confidence limits, then it indicates the observed phase angle difference goes beyond a normal condition.

Although a powerful tool, a fixed KPCA model may lead to excessive false alarms, since power systems are time-varying in nature, influenced by load fluctuation, uncertainty in power flow, network topology and intermittency of certain types of renewable generation. To tackle this problem, a moving window approach is adopted to update the KPCA model.

B. Implementation

The implementation of the moving window KPCA-based islanding protection method is summarized in Fig. 1. It involves two steps:

1) Phase angle data is collected and sent to a central control centre or a substation, where an offline KPCA model is constructed using the angle difference data across different sites to obtain the initial PCs and initial control limits; and

2) Online updating of the KPCA model and evaluation of T^2 and Q for each new data point to determine if control limits are exceeded, necessitating the triggering of islanding protection relays. The detection time for the proposed method is calculated as $T = T_{cal} + T_D + T_{com}$, where T_{cal} is the $O(N^3)$ computation time of the proposed algorithm, where N is the window size; T_D is a time delay of a few hundred milliseconds to avoid false operation introduced by measurement error etc.; and T_{com} is the latency of two-way communication, which is normally between 20 and 200 milliseconds [35]. In general, a response time of less than 2 s is achievable to meet the IEEE standard [36]. If the communication link is down or communication latencies are high, conventional islanding protection methods, which rely only on localized measurement, can be used as a backup.

It should be noted that the number of retained kernel PCs r may vary over time and need to be adaptively determined. Numerous methods have been proposed in the literature to determine r, such as the cumulative percent variance [37], scree test [38], average eigenvalues, imbedded error function [38], and Akaike information criterion [39]. In this paper, the intuitive cumulative percent variance approach was used to determine the number of PCs.

III. Evaluation using Simulated synthetic Data

In order to test the proposed islanding detection approach for different types of power system event the IEEE Nine-bus System, described in [40], is used as a test network for dynamic simulation. Fig. 2 shows the single line diagram of the network, which is modelled and available in the DigSilent PowerFactory Version 15.2.1. Consider a PMU is installed at each bus, and records data with a sampling rate of 10 Hz.

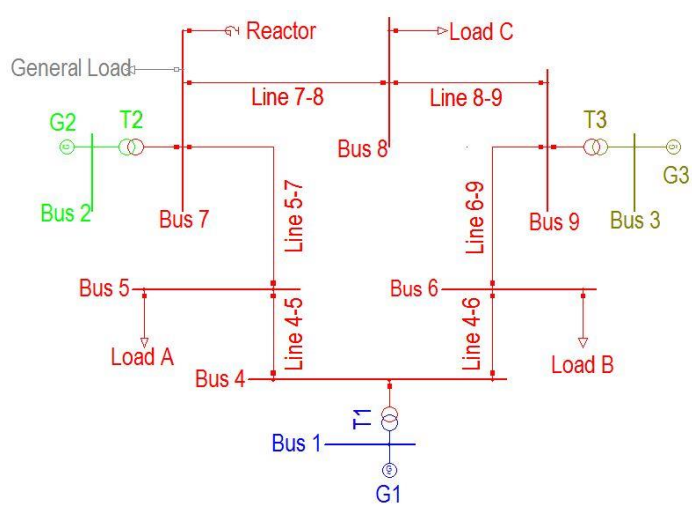

Fig. 2. IEEE Nine-bus System test network

The generators G1, G2 & G3 use both the TGOV1 steam turbine governor model, and the standard IEEET1 AVR model. The loads A, B & C are modified to incorporate a Gaussian noise component to mimic the real system load. Load A ramps up, while loads B & C remain constant.

A. *Determination of a KPCA model*

The construction of a moving window KPCA model involves the selection of a kernel parameter, σ, the window length, *N*, the initial number of principal components, *r*, and the delay for applying the adaptive KPCA model, *l* [23].

As recommended in reference [19], a Gaussian kernel function is used for model construction. From the above Nine-bus System, a data set of 1500 samples with normal conditions was generated. Fig. 3(a) upper plot shows the number of non-zero eigenvalues *p* versus the kernel parameter σ. The larger the σ, the fewer retained KPCs are required to reconstruct the kernel matrix. Fig. 3(a) lower plot shows the variance captured versus the retained KPCs. With σ=20 for example, for window size *N* =200, only 100 out of 200 eigenvalues are non-zero [Fig.3(a) upper plot] and only 20 out of 100 non-zeros are significant, which captured about 80% variance of the kernel matrix [Fig. 3(a) lower plot]. Inspecting the adaptation performance of the proposed approach, revealed that a window size of *N*=200 was able to adapt the changes in the phase angle. A small window size led to an increase in the false detection, while a larger window size resulted in an increase in the missing alarms [Fig. 3(b)].

(a)

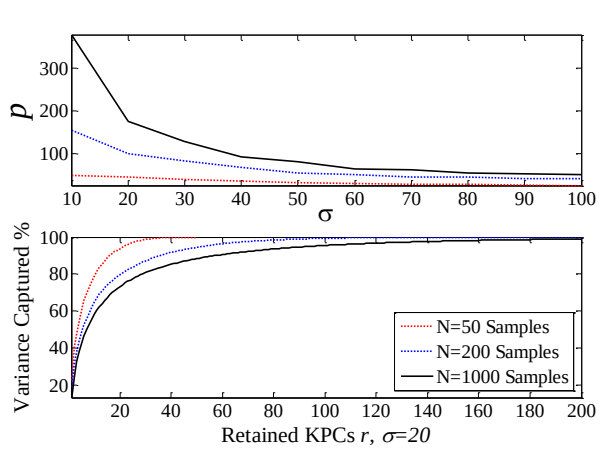

(b)

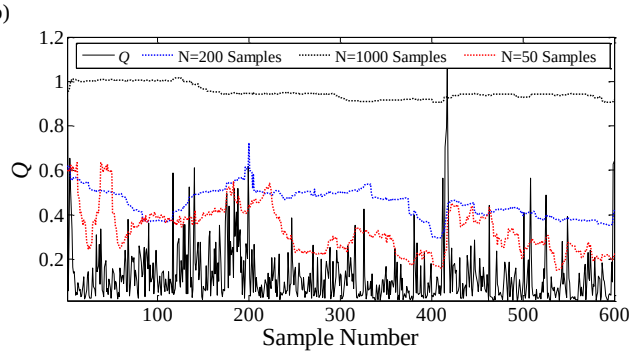

Fig. 3. (a) Kernel parameter *σ* with the number of non-zero eigenvalues *p* (upper plot); variance captured with retained initial KPCs *r*, for σ=20 (lower plot); (b) adaptive *Q* statistic for normal data, with window size 50 (red dashed line), 200 (blue dashed line) and 1000 (solid line).

Other parameters are set to be σ=20, initial *r* =20, and delay *l* =40 for a 99.9% confidence limit.

B. *Detection Results for the Simulated Nine-Bus System*

Three different classes of events are simulated for evaluation: Case 1 – Generator Trip; Case 2 – Islanding with large frequency change; and Case 3 – Islanding with small frequency change.

1) *Generator Trip*

In Case 1, Generator G1 trips from 51 MW at *t=500 samples* resulting in a lower steady state frequency. Generators G2 & G3 increase output corresponding to a 4% droop. Fig. 4 upper plot shows how the phase angles for bus 5, bus 7 & bus 9 change during the disturbance. No islands are created in Case 1. Fig. 4 lower plot shows the detection result for this event, where only 4 samples are above the 99.9% confidence limit at *t=503-506* samples, lasting 400 ms. In practice, a 500 ms delay is deliberately introduced, to avoid false triggers.

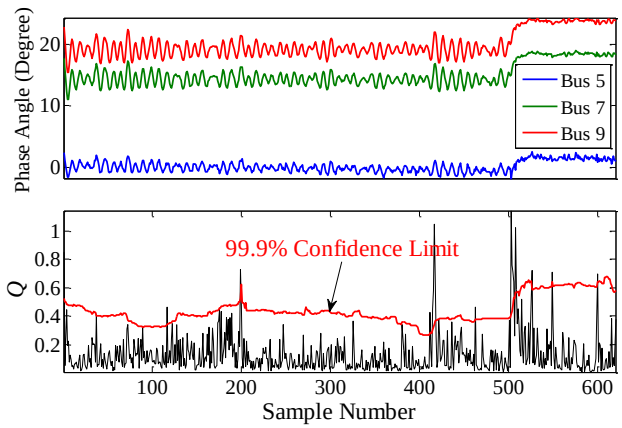

Fig. 4. Case 1 Generator G1 Trip at 500 samples

2) *Islanding with large frequency change*

Fig. 5 depicts Case 2 in which Bus 1, Bus 4 and Bus 6 separate from the rest of the network and form an island. Line 6-9 is already open at Bus 6 (typical for circuit breaker maintenance, etc.) and then Line 4-5 disconnects from Bus 5 at *t=400 samples*. Line 4-5 has a Flow of 20 MW towards bus 4 immediately prior to the island forming.

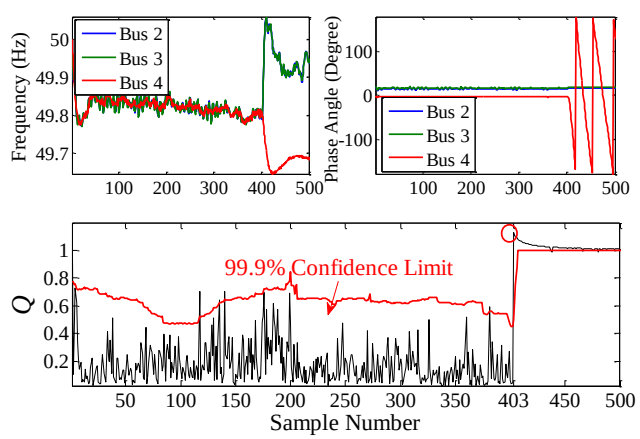

Fig. 5. Case 2 Islanding with Large frequency change

The voltage angle of the island at Bus 4 (Fig. 5, upper right plot) deviates quickly from the main network and continually drifts due to the large difference in system frequencies. An island is clearly evident in both frequency and phase angle. Fig. 5 lower plot shows the detection result for Case 2. The Q statistic detects the islanding event successfully after the 403 samples (i.e. 300 ms after the islanding event occurred).

3) Islanding with small frequency change

Fig. 6 depicts Case 3 in which Bus 1, Bus 4 & Bus 6 again separate from the rest of the network and form an island. Line 6-9 is open at Bus 6 and Line 4-5 disconnects from Bus 5 at *t=400 samples*. In this case there is only a small flow of 1 MW towards bus 4 immediately prior to the island forming. After the island forms the frequency of G2 and G3 do not substantially deviate from the frequency of G1 in the island. Fig. 6 upper right plot shows how the phase angle of the island does, however continually drift from the main network indicating a change in topology. Clearly, Fig. 6 lower left plot shows how examination of frequency only, proposed in [4], is insufficient to identify islands in this case. Specifically, the $Q_{frequency}$ only detects the event at the *t=419-423* samples, i.e. 1.9 s delay after the event occurred, and only for a duration of 400 ms. Again, the Q statistic of the proposed approach detects the islanding event successfully after the 403 samples (i.e. 300 ms after islanding event occurred). In comparison, the change of angle difference approach proposed in [6], which sets the threshold of the change of angle difference to be 30 degrees, can only detect the events after the 431 sample, with a delay of 3.1 s. It is clear that both methods proposed in [4] and [6] fail to detect the islanding event successfully within 2 s to meet the IEEE standard 1547-2003[36].

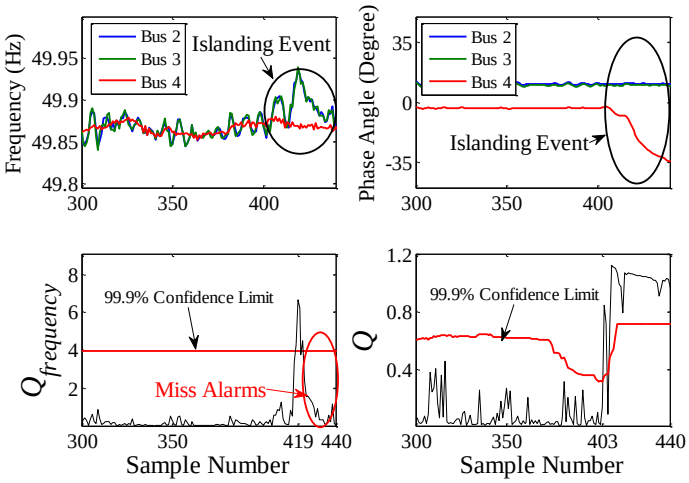

Fig. 6. Case 3 Islanding with small frequency change.

IV. Industrial Multivariate Phase Angle Data

A. Wide Area Phase Angle Difference Data from the GB and the Irish Power System

The proposed method is demonstrated using data collected between 2012 and 2015, from the GB and the Irish (NI & RoI) power grid through the OpenPMU project [35]. The GB system is linked with the Irish power system via a 500 MW HVDC link to NI & a 500 MW HVDC link to RoI. The French system is linked to the GB system via a 2000 MW

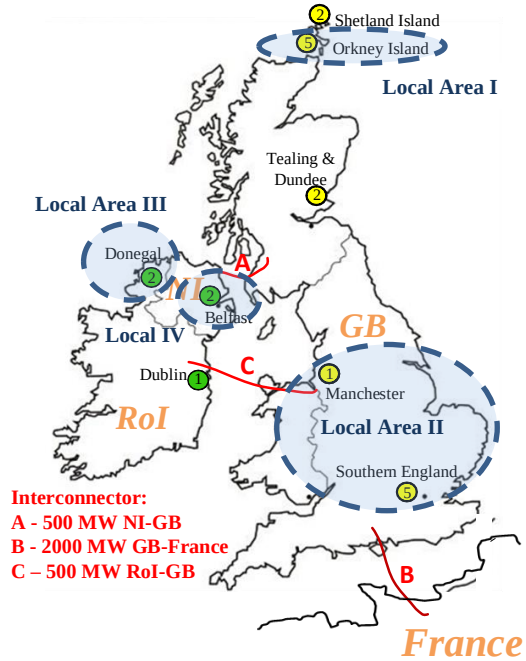

Fig. 7. OpenPMU layout in the GB and Irish networks. The number of PMUs installed at the various locations is represented by the number in the circles. The Green one belongs to the Irish system and the yellow one the GB system.

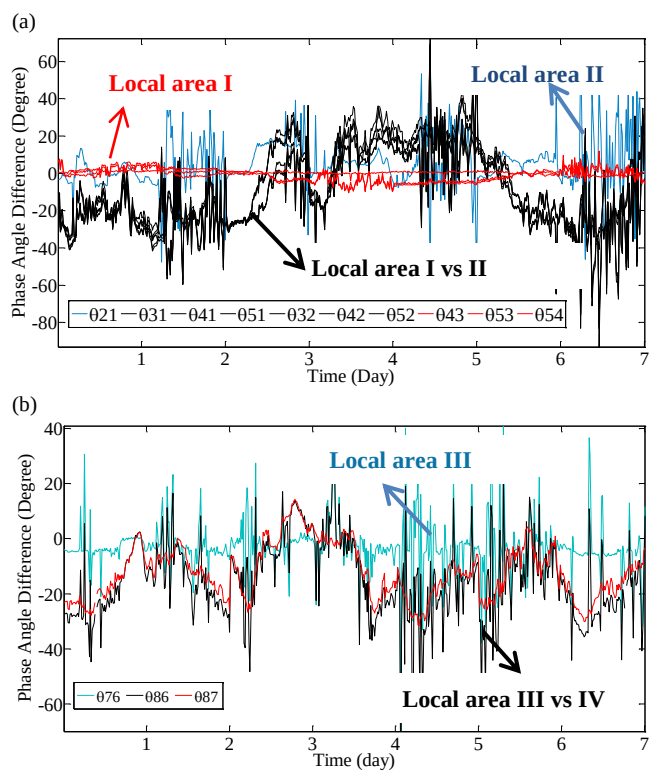

Fig. 8. Variation of phase angle difference under normal operation: (a) across 5 sites for the GB system; (b) across 3 sites for Irish system.

HVDC interconnector. PMUs, developed at Queen's University Belfast and supported by Scottish and Southern Energy Ltd., were installed across the GB, NI and RoI power systems. The locations of the PMUs are illustrated in Fig. 7.

TABLE I
COMPARATIVE ANALYSIS OF PHASE ANGLE BASED METHODS, CONVENTIONAL ROCOF, VECTOR SHIFT

Single Reference		Local Area based	Wide Area based
	Characteristic	Small variation	Large variation
	Advantages	Low computation cost; fast operation	
	Disadvantages	○ Relying on a single reference and ill-suited if the reference signal is problematic, e.g., nosiy signal, loss of communication, or also become islanded. ○ Location of reference requires careful consideration. ○ Fixed threshold results in large non-detection zone or false operation.	
Multiple References	Characteristic	Small variation	Large variation
	Advantages	○ More robust in comparison to single reference. ○ Easy to integrate with multivariate statistical analysis, capable of handling noisy data.	
		○ For a fixed threshold method, have a tighter control limit and may be more sensitive compared with the wide area based approach.	○ Ultimately making use of the information available in a systematic wide area; more robust in comparison to single reference based and 'local area' based approach. ○ No prior network knowledge is required.
	Disadvantages	○ Unaware of the situation in a wider area. ○ Ill-suited if the local area is synchronously islanded. ○ The concept of local area needs to be carefully examined. May require prior network knowledge.	○ Significant time-varying characteristic and large variation magnitude requires sophisticated model. ○ High computation and communication cost.
ROCOF	Advantages	Low computation cost; fast operation	N/A
Vector Shift	Disadvantages	○ Unaware of the situation in a wider area. ○ Prone to false operation during large network disturbances, especially for low inertia systems	N/A

For the GB system, phase angle data measured from 5 sites were analyzed, including $\boldsymbol{\theta}_1$ (Southern England), $\boldsymbol{\theta}_2$ (Manchester), $\boldsymbol{\theta}_3, \boldsymbol{\theta}_4, \boldsymbol{\theta}_5$ (Orkney Islands). This results in 10 phase angle difference variables, $\boldsymbol{\theta}_{ji} = \boldsymbol{\theta}_j - \boldsymbol{\theta}_i$, where $i, j \in \{1, 2, \ldots, 5\}, i \neq j$. For the Irish system (including NI and RoI), the analyzed data set consists of phase angles from 3 sites, with $\boldsymbol{\theta}_6$, $\boldsymbol{\theta}_7$ (Donegal), and $\boldsymbol{\theta}_8$ (QUB), which produces 3 phase angle difference variables, $\boldsymbol{\theta}_{76}$, $\boldsymbol{\theta}_{86}$, and $\boldsymbol{\theta}_{87}$. All the data studied in this paper have a sampling rate of 10 Hz.

Seven days of synchronously recorded angle data under normal operating conditions were arbitrarily chosen to illustrate the variation of the angle difference, across different sites. Fig. 8(a) and Fig. 8(b) represent the GB system, including local area I (Orkney Island) and II (Manchester, Southern England) and the separate Irish system, including local area III (Donegal), and IV (Belfast), respectively.

B. Comparative Analysis of Angle Difference Based Methods, Conventional RoCoF and Vector Shift

Before demonstrating the effectiveness of the proposed scheme for islanding protection, the advantages and disadvantages of different methodologies based on angle difference, conventional RoCoF and vector shift, are discussed with regard to their reliability, sensitivity and computational cost, and presented in Table I. Angle difference based approaches can be divided into the following categories:

(1) 'Single reference approach': This is well established in the literature [6], [9], [27]. However, it is worth noting that the angle difference variation depends on the location of the chosen 'single reference'. If the angle signals belong to the same local area, the variation of the angle difference is small (e.g. Fig. 8(a), the red lines $\boldsymbol{\theta}_{43}, \boldsymbol{\theta}_{53}, \boldsymbol{\theta}_{54}$ representing reference signals at the same local area), otherwise, the variation of the angle difference is large (e.g. Fig. 8(a), the black lines $\boldsymbol{\theta}_{31}, \boldsymbol{\theta}_{41}, \boldsymbol{\theta}_{51}, \boldsymbol{\theta}_{32}, \boldsymbol{\theta}_{42}, \boldsymbol{\theta}_{52}$ represent reference signals at different local areas). In this context, the 'single reference approach' can be further classified as a 'local area' or a 'wide area' based method (Table I).

(2) 'Local area multiple references approach': In this paper, the use of multiple local references within the same area is referred to as a 'local area' based 'multiple cross reference' approach. For example, in Fig. 8(a), the red lines $\boldsymbol{\theta}_{43}, \boldsymbol{\theta}_{53}, \boldsymbol{\theta}_{54}$ represent reference signals at the same local area. However, the concept of 'local area' needs to be carefully examined and may require prior network knowledge. This is rather complex and deserve further investigation in a full paper.

(3) 'Wide area multiple references approach': This refers to a 'multiple cross reference', 'wide area' based methodology, where the references are across a wide area.

The methodology of the proposed 'wide area multiple references approach' will be explored and examined in detail in the next section. More specifically, the 10 signals in Fig. 8(a) or the 3 signals in Fig. 8(b) will be analysed simultaneously to provide an adaptive threshold, with the aid of a moving window Kernel PCA approach. It is worth mentioning that the traditional RoCoF and vector shift approaches essentially rely on local data and ignore the valuable information in a wider area.

V. Islanding Detection Results

A. Construction of a Moving Window KPCA Model

As before, the construction of a moving window KPCA model involves the selection of a kernel parameter, σ, the window length, N, the initial number of principal components, r, and the delay for applying the adaptive KPCA model, l. Varying the window size from $N = 1$ hour to $N = 24$ hours suggested that $N = 2$ hours could adapt to the time-varying characteristics in the variable interrelationships within the reference angle difference data set. A tradeoff between the window size and algorithm sensitivity has to be carefully balanced. Parameters of the KPCA models for both the GB and Irish systems are selected as shown in Table II.

TABLE II
Moving Window KPCA Model Parameters for GB and Irish Systems

	σ	N	r	l
GB System	400	2 hours	3	40
Irish System	20	2 hours	2	40

B. Comparison with Other Islanding Detection Methods

In order to demonstrate the performance of the proposed scheme and its effectiveness, it is compared with other islanding detection methods, including RoCoF, angle difference, linear PCA, and nonlinear Kernel PCA. The angle difference data under normal operation conditions, shown in Fig. 8(a), were used for analysis. The first six-days data were used as reference, and the seventh-day for testing. Table III summarizes the false alarm rates from the five different methods. A 95% confidence level (CL) was used for the angle difference, PCA, Kernel PCA, and moving window KPCA models. The result implies that the false alarm rates for the PCA, Kernel PCA, and angle difference approach for ($\boldsymbol{\theta}_{21}$) are significantly higher than expected (5%). This would imply oversensitivity for detecting islanding.

TABLE III
False Alarm Rates for Reference Data by RoCoF, Angle Difference, PCA, Kernel PCA, Moving Window KPCA.

Method		Model Parameter		False Alarm Rates
RoCoF (over 50 cycles)		threshold =0.125 Hz/second		0%
Angle Difference	$\boldsymbol{\theta}_{21}$	threshold = 24	Based on 2 $\bar{\sigma}$ rule, $\bar{\sigma}$ is standard deviation	18.97%
	$\boldsymbol{\theta}_{31}$	threshold = 44		0%
	$\boldsymbol{\theta}_{43}$	threshold = 7		1.12%
PCA		r = 1 PC		74.46%
Kernel PCA		σ=20, r =5 PCs		15.14%
Moving window KPCA		As shown in Table I		8.23%

C. Detection Results for Inter-connector trip and Islanding Events in the GB system

On the morning of 28 September 2012, an inter-connector trip event occurred on the HVDC link between GB and France, resulting in disconnection of a 1 GW infeed. The resulting rate-of-change of frequency, -0.186 Hz/second (calculated over 50 cycles) at one particular GB site, exceeded the RoCoF setting of -0.125 Hz/second, and triggered the associated islanding protection, even though local islanding had not occurred. This highlights the limitations of conventional islanding protection techniques and the inability to discriminate between real islanding conditions and wide spread power system disturbances. This is clearly a concern for safety and system stability which is likely to escalate in future with the much anticipated greater levels of HVDC interconnection.

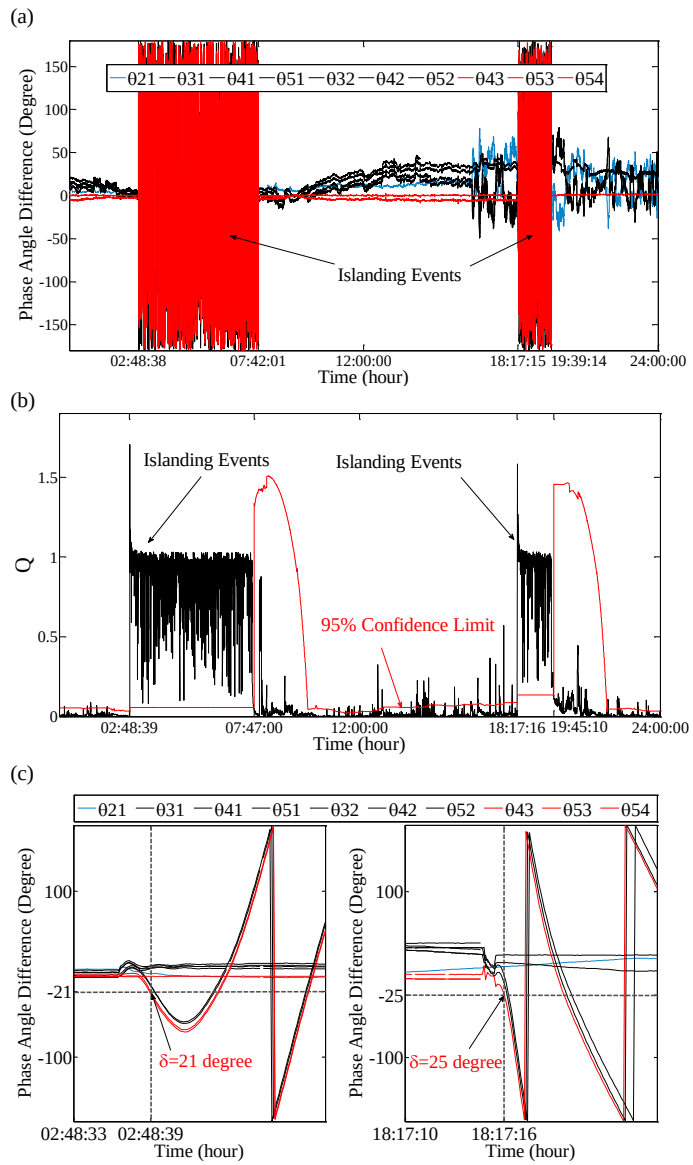

Fig. 9. 28 September 2012 case study: (a) Phase angle difference across 5 different sites in the GB system; (b) detection results using moving window KPCA with a 95% confidence limit; (c) magnified view of detection results at 02:48 and 18:17.

The phase angle difference among 5 sites is illustrated in Fig. 9(a) for this event. When the GB-France inter-connector tripped at 02:48:38, the phase angle of an islanded site, relative to the main grid, drifts for approximately 5 hours. A similar event occurred in the evening, when the GB-France inter-connector tripped again at 18:17:15, and an island occurred and existed for more than 1 hour. The 28 September

2012 islanding events have been well documented in the literature [4],[7],[9],[33] and in National Grid publications. It provides a useful benchmark case study. Therefore, the event is presented here again, facilitating comparison with the PCA frequency-based islanding detection approach presented in [4].

Fig. 9(b) illustrates the application of the adaptive kernel PCA-based detection technique to the phase angle difference data set. The islanding events can be clearly detected by the Q statistic from 02:48:39 and from 18:17:16. The magnified view in Fig. 9(c) indicates that at 02:48:39 the threshold of angle difference is 21 degree, while at 18:17:16 the threshold has adaptively changed to be 25 degree for effective islanding detection. The case study reveals that the proposed method is more reliable than conventional RoCoF which triggered inappropriately. Unlike the PCA method for wide-area frequency analysis presented in [7], the proposed method does not have a non-detection zone, though this comes at the expense of greater computation complexity.

D. Detection Results for Generation Trip and Inter-connector Trip Events in the Irish system

In 2012, an RoI-GB inter-connector trip event occurred at 21:14:50, and the Irish power system frequency went from 49.85 Hz to 50.43 Hz in 10 seconds. In the same evening, a generator tripped at 23:10:12, causing a low frequency event, with a frequency nadir of 49.85 Hz.

The 24-hour frequency and phase angle difference variations across different sites in the Irish system are shown

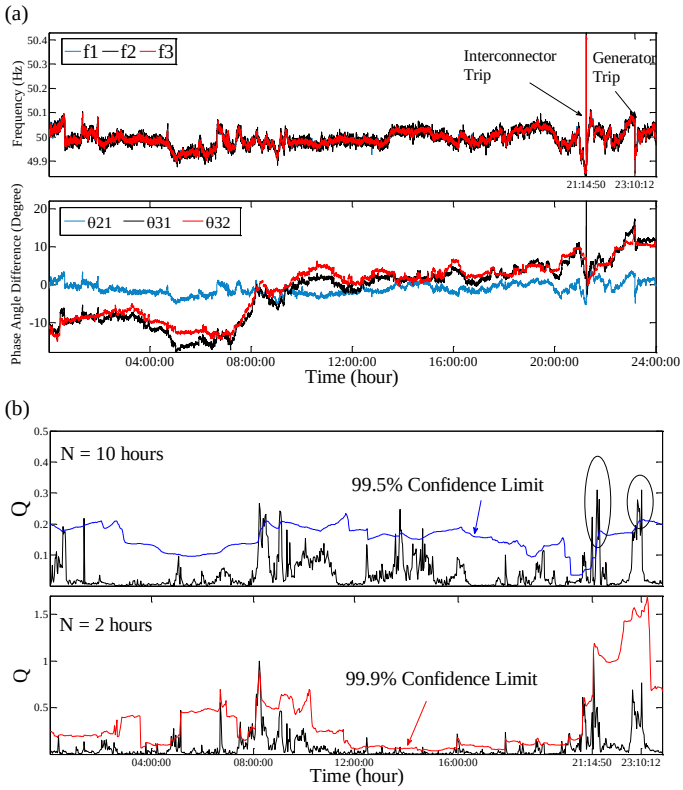

Fig. 10. (a) Frequency variation indicating generation trip and interconnector trip events (upper plot); Phase angle difference across different sites in the Irish system (lower plot); (b) detection result using moving window KPCA with two different window sizes and confidence limits.

TABLE IV
ISLANDING DETECTION RESULSTS FOR SAMPLE TEST CASES OF ISLANDING AND NON-ISLANDING EVENTS FROM THE GB AND IRELAND POWER SYSTEMS

	Test Cases	Year /System	Frequency (Hz)	Missing/ False alarm rates
1	Interconnector trip&islanding	2012 /GB	49.97-49.6	Missing alarm: 0% & 80% for 95% & 99.9% confidence limit
2	Trip&islanding		49.93-48.7	
3	Islanding	2014 /GB	49.8 vs 50.0	
4	Islanding		49.83 vs 50.05	
5	Islanding		49.9 vs 50	
6	High frequency	2014 /GB	49.97-50.3	False alarm: 8.2% & 2.1% for 95% & 99.9% confidence limit
7	High frequency		49.9-49.7	
8	Low & high frequency		49.9-49.66-50.22	
9	High frequency		50-50.3	
10	Normal operation		49.8-50.2	
11	Unit trip	2012 /Ireland	50-49.5	False alarm: 4.4% & 1.6% for 95% & 99.9% confidence limit
12	Unit trip		50-49.88	
13	Unit trip		50-49.85	
14	Interconnector trip		49.85-50.2	
15	High & low frequency		50.09-50.27-49.76	
16	Unit trip		50.1-50.3-49.75	
17	Normal operation		49.85-50.15	

in Fig. 10(a) upper plot and lower plot, respectively. Fig. 10(b) illustrates the detection results of the phase angle difference data for a window size of 10 hours with a 99.5% CL (upper plot), and a window size of 2 hours with a 99.9% CL (lower plot), respectively. It is clear in each case when the inter-connector and generator trips occur and that for a window size of $N = 2$ hours with a 99.9% CL incorrect triggering of islanding protection relays is avoided.

The proposed method has been further examined and validated for other test cases randomly selected from the GB and Ireland power systems, as reported in Table IV. As shown, the sensitivity of the propose method can be adjusted by changing the confidence limit level.

VI. DISCUSSION AND CONCLUSIONS

This paper presented a novel technique for anti-islanding protection based on analyzing the phase angle difference from multiple locations simultaneously. The effectiveness of the proposed method using adaptive kernel PCA was verified by both DigSilent simulated cases and real cases recorded from two independent power systems. Comparative analysis between the proposed and existing state-of-the-art methods, including RoCoF, phase angle difference between two locations, PCA, and Kernel PCA based methods revealed that the proposed method has superior reliability due to the adaptive protection strategy. This approach provides a powerful tool for analyzing phase angle measurements from

multiple locations simultaneously, enabling the development of a systematic, system-independent adaptive protection scheme for wide area anti-islanding protection.

By combining the frequency-based method presented in our previous work [4], with the proposed phase angle based approach, the speed and reliability of islanding detection can be substantially improved. In particular, the non-detection zone issue associated with the frequency based approach is mitigated as phase angle difference between islanded systems drifts even when the frequency mismatch is very small.

The limitation of this approach is if the phase angles in the islanding system are well matched with those of other sites, it will fail to detect islanding successfully. In addition, it would be useful to investigate an extended KPCA algorithm to improve detection robustness with respect to noise, incorrect measurements and outliers. This will be addressed in future work.

REFERENCES

[1] Renewables 2014: Global Status Report: REN 21. www.ren21.net

[2] J. O'Sullivan, A. Rogers, D. Flynn, P. Smith, A. Mullane, M. O'Malley, "Studying the maximum instantaneous non-synchronous generation in an island system – frequency stability challenges in Ireland," *IEEE Trans. Power Syst.*, vol. 29, no. 6, pp. 2943–2951, Nov. 2014.

[3] P. Mahat, Z. Chen, and B. Bak-Jensen, "Review on islanding operation of distribution system with distributed generation," in *Proc. IEEE Power Energy Soc. Gen. Meeting*, 2011, pp. 1–8.

[4] X. Liu, D. Laverty, R. Best, K. Li, D.J. Morrow and S. McLoone, "Principal component analysis of wide area phasor measurements for islanding detection - a geometric view," *IEEE Trans. Power Del.*, vol. 30, no. 2, pp. 976–985, Apr. 2015.

[5] Yip, H.T.; Millar, G.; Lloyd, G.J.; Dysko, A.; Burt, G.M.; Tumilty, R., "Islanding detection using an accumulated phase angle drift measurement," *in Proc. 10th IET Int. Devel. Power Syst. Protec. (DPSP 2010)*, 2010, pp.1–5.

[6] Z. Lin, T. Xia, Y. Ye, Y. Zhang, L. Chen, Y. Liu, K. Tomsovic, T. Bilke, and F.Wen, "Application of wide area measurement systems to islanding detection of bulk power systems," *IEEE Trans. Power Syst.*, vol. 28, no. 2, pp. 2006–2015, May 2013.

[7] X. Liu, D. Laverty, and R. Best, "Islanding Detection Based on Probabilistic PCA with Missing Values in PMU Data," in *Proc. IEEE Power Energy Soc. Gen. Meeting*, 2014, pp. 1–6.

[8] Y Guo, K. Li, D. Laverty, "Synchrophasor-based islanding detection for distributed generation systems using systematic principal component analysis approaches," *IEEE Trans. Power Del.*,DOI10.1109/TPWRD. 2015.243515.

[9] L. Xie, Y. Chen and P. R. Kumar, "Dimensionality reduction of synchrophasor data for early event detection: linearized analysis," *IEEE Trans. Power Syst.*, vol. 29, no. 6, pp. 2784–2794, 2014.

[10] D.J. Burke, M. O'Malley, "A study of principal component analysis applied to spatially distributed wind power," *IEEE Trans. Power Syst.*, vol. 26, no. 4, pp. 2084–2092, Nov. 2011.

[11] E. Barocio, E., B.C. Pal, D. Fabozzi, and N.F. Thornhill, N.F. "Detection and visualization of power system disturbances using principal component analysis," *in Proc. IREP*, 2013, pp.1–10.

[12] A. Krishna, B. Chaudhuri, N. Thornhill, and B. C. Pal, "Coherency identification in power systems through principal component analysis," *IEEE Trans. Power Syst.*, vol. 20, no. 3, pp. 1658-1660, Aug. 2005.

[13] M. Ariff and B. C. Pal, "Coherency identification in interconnected power system - an independent component analysis approach," *IEEE Trans. Power Syst.*, vol. 28, no. 2, pp. 1747–1756, May 2013.

[14] J. Thambirajah, N. F. Thornhill, B. C. Pal, "A multivariate approach towards inter-area oscillation damping estimation under ambient conditions via independent component analysis and random decrement," *IEEE Trans. Power Syst.*, vol. 26, no. 1, pp. 315–322, Feb. 2011.

[15] M. Rafferty, X. Liu, S. McLoone, "Real-time multiple events detection and isolation using moving window PCA," submitted to *IEEE Trans. Smart Grid*, 2015.

[16] D.J.H. Wilson, G.W. Irwin, G. Lightbody, "RBF principal manifolds for process monitoring," *IEEE Trans. Neural Netw.*, vol. 10, no. 6, pp. 1424–1434, Nov. 1999.

[17] M.A. Kramer, "Nonlinear principal component analysis using auto-associative neural networks," *AIChE J.*, vol. 37, no. 3, pp. 233–243 Feb.1991.

[18] B. Scholkopf, A.J. Smola, K.R. Muller, "Nonlinear component analysis as a kernel eigenvalue problem," *Neural Comput*., vol. 10, no. 5, pp. 1299–1319, Jul. 1998.

[19] B. Scholkopf, S. Mika, C.J.C. Burges, P. Knirsch, K.R. Muller, "Input space versus feature space in kernel-based methods," *IEEE Trans. Neural Netw.*, vol. 10, no. 5, pp. 1000–1016, 1999.

[20] X. Wang, U. Kruger, B. Lennox, B., "Recursive partial least squares algorithms for monitoring complex industrial processes," *Control Eng. Pract*., vol. 11, no. 6, pp. 613–632, June, 2003.

[21] W. Li, H. Yue, S. Valle-Cervantes, S.J. Qin, "Recursive PCA for adaptive process monitoring," *J. Process Contr*, vol. 10, no. 5, pp. 471–486, Oct., 2000.

[22] L. Hoegaerts, L.D. Lathauwer, I. Goethals, "Efficiently updating and tracking the dominant kernel principal components," *Neural Netw*., vol. 20, no. 2, pp. 220–229, Mar., 2007.

[23] X. Liu, U. Kruger, T. Littler, L. Xie, and S. Wang, "Moving window kernel PCA for adaptive monitoring of nonlinear processes," *Chemometr. Intell. Lab.*, vol. 96, no. 2, pp. 132–143, 2009.

[24] E. Barocio, B.C. Pal, N.F. Thornhill, A.R. Messina, "A dynamic mode decomposition framework for global power system oscillation analysis," *IEEE Trans. Power Syst.*, vol.30, no.6, pp.2902-2912, Nov. 2015.

[25] X. Ding, .A. Crossley, D.J. Morrow, "Islanding detection for distributed generation," *JEET*, vol.2, no.1, pp.19-28, 2007.

[26] D. M. Laverty, R. J. Best, and D. J. Morrow, "Loss-of-mains protection system by application of phasor measurement unit technology with experimentally assessed threshold settings," *IET Gener, Transm Dis*, pp. 146–153, Jan. 2015.

[27] Ohno, T.; Yasuda, T.; Takahashi, O.; Kaminaga, M.; Imai, S., "Islanding protection system based on synchronized phasor measurements and its operational experiences," in *Proc. IEEE Power Energy Soc. Gen. Meeting*, 2008, pp. 1–5.

[28] N. W. A. Lidula, N. Perera, and A. Rajapakse, "Investigation of a fast islanding detection methodology using transient signals," in *Proc. IEEE Power Energy Soc. Gen. Meeting*, 2009, pp. 1–6.

[29] W. Najy, H. Zeineldin, A. Alaboudy, and W.-L. Woon, "A Bayesian passive islanding detection method for inverter-based distributed generation using esprit," *IEEE Trans. Power Del*., vol. 26, no. 4, pp. 2687–2696, Oct. 2011.

[30] S. R. Samantaray, K. El-Arroudi, G. Joos, and I. Kamwa, "A fuzzy rule-based approach for islanding detection in distributed generation," *IEEE Trans. Power Del.*, vol. 25, no. 3, pp. 1427–1433, Jul. 2010.

[31] K. El-Arroudi, G. Joos, I. Kamwa, and D. McGillis, "Intelligent-based approach to islanding detection in distributed generation," *IEEE Trans. Power Del.*, vol. 22, no. 2, pp. 828–835, Apr. 2007.

[32] K. El-Arroudi and G. Joos, "Data mining approach to threshold settings of islanding relays in distributed generation," *IEEE Trans. Power Syst.*, vol. 22, no. 3, pp. 1112–1119, Aug. 2007.

[33] Lloyd, G.; Hosseini, S.; Chang An; Chamberlain, M.; Dysko, A.; Malone, F., "Experience with accumulated phase angle drift measurement for islanding detection," *in Proc. 22nd Int. Conf. Electr. Dis.(CIRED 2013)*, 2013, pp.1–4.

[34] Jackson, J.E., *A User's Guide to Principal Components*. 1991, New York: Wiley Inter-science.

[35] D. Laverty, R. Best, P. Brogan, I. Al Khatib, L. Vanfretti, and D. Morrow, "The OpenPMU platform for open-source phasor measurements," *IEEE Trans. Instrum. Meas.*, vol. 62, no. 4, pp.701–709, Apr. 2013.

[36] *Standard for Interconnecting Distributed Resources With Electric Power Systems*, IEEE Standard 1547, 2003.

[37] F.R. Malinowski, *Factor Analysis in Chemistry*. 1991, New York: Wiley.

[38] R.B. Cattell, "The scree test for the number of factor," *Multivar. Behav. Res.*, vol. 1, no. 2, pp.245–276, 1966.

[39] H. Akaike, "A new look at the statistical model identification," *IEEE Trans. Autom.Control*, vol. 19, no. 6, pp.716–723, Dec. 1974.

[40] P. Anderson and A. Fouad, Power SystemControl and Stability, 1st ed. Iowa State University Press, Ames, Iowa, U.S.A., 1977.